Improved double extended octagonal ring drawbar transducer for 3-D force measurement

N.B. McLAUGHLIN[1], S. TESSIER[2] and A. GUILBERT[3]

[1]Eastern Cereal and Oilseed Research Centre, Research Branch, Agriculture and Agri-Food Canada, Ottawa, ON, Canada K1A 0C6; [2]Animal Industry Branch, Manitoba Agriculture, 204-545 University Crescent, Winnipeg, MB, Canada R3T 5S6; and [3]Département de des sols et de génie agroalimentaire, FSAA, Université Laval, Québec, QC, Canada G1K 7P4. *Received 13 March 1998; accepted 1 December 1998.*

McLaughlin, N.B., Tessier, S. and Guilbert, A. 1998. **Improved double extended octagonal ring drawbar transducer for 3-D force measurement.** Can. Agric. Eng. **40**:257-264. A double extended octagonal ring (DEOR) drawbar force transducer is presented. This transducer utilizes two extended octagonal ring (EOR) transducers one located on each side of the drawbar to measure drawbar draft and vertical and side loads with minimum alteration of the tractor-implement hitch point configuration. Side loads are derived from the differential draft outputs of the two EOR's. The transducer was calibrated in a special calibration jig capable of simultaneously and independently applying draft, vertical, and side loads. The DEOR exhibited excellent linearity with draft and vertical sensitivities of 98.0 and 94.8 $\mu V\ V^{-1}\ kN^{-1}$, respectively. Cross-sensitivity ranged between 2 and 7% of the primary DEOR output. Including cross sensitivity in the predictive force equations derived from multiple regression on 3-D calibration data compensated for this systematic error. The DEOR dynamometer was used to measure drawbar force components of secondary tillage tools in an on-farm research program. The portable device proved to be very sensitive, versatile, and suitable for measuring draft and moderate vertical and side drawbar forces exerted by most pull-type implement hitch configurations. **Keywords**: strain gage, extended octagonal ring, cross sensitivity, draft.

On présente ici un transducteur à double bague octogonale allongée (DEOR) pour mesurer la force sur la barre de traction. Ce transducteur utilise deux transducteurs à bague octogonale allongée (EOR), un de chaque côté de la barre de traction pour mesurer l'effort de traction à la barre et les charges verticales et latérales, en modifiant au minimum la configuration du point d'attelage tracteur-outil. Les charges latérales sont dérivées de la différence entre les forces de traction à la sortie des deux bagues. Le transducteur a été calibré avec une jauge de calibration spéciale capable d'appliquer, de manière simultanée et indépendante, une force de traction et des charges verticales et latérales. La double bague (DEOR) a montré une excellente linéarité et les sensibilités verticales et en traction étaient de 98.0 et 94.8 $\mu V\ V^{-1}\ kN^{-1}$, respectivement. La sensibilité croisée était de 2 à 7% de la force de traction primaire à la sortie de la double bague (DEOR). L'inclusion de la sensibilité croisée dans les équations de force obtenues grâce à des régressions multiples des données de calibration tri-dimensionnelles a permis de compenser pour cette erreur systématique. Dans le cadre d'un programme de recherche à la ferme, le dynamomètre à double bague a été utilisé pour mesurer les composantes de la force de traction à la barre de plusieurs outils de travail du sol. L'appareil de mesure portatif a démontré sa sensibilité, sa versatilité et sa capacité de mesurer la traction et les forces de traction à la barre modérées, verticales et latérales, qu'exercent la plupart des outils lorsqu'ils sont tirés. **Mots-clés**: jauge de contrainte, bague octogonale allongée, sensibilité croisée, traction.

INTRODUCTION

Soil compaction by heavy agricultural equipment is among the most important soil degradation agents in Eastern Canada and North Eastern United States. Wheel induced soil compaction arising from field traffic with heavy wagons, tankers, and harvesting equipment has been well established (Tessier et al. 1991) and is quite predictable (Chi et al. 1991; Plouffe et al. 1994). Tractor wheel traffic may account for up to 90% of the surface wheel traffic (Hånkasson et al. 1988; Raghavan and McKyes 1990). As a consequence, soil compaction has become the leading cause of soil degradation in long growing season crops such as grain corn, where producers are often forced to perform primary tillage in late fall under very moist soil conditions.

Proper matching of tractor and implement size can contribute to a reduction in soil compaction. Reducing tractor size to match implement width results in lower tractor weight, while increasing implement width to match available tractor power reduces wheel traffic. Québec agricultural engineers and extension specialists have relied on the *Comité de références économiques en agriculture du Québec* (CREAQ 1991) economic data reports which present and summarize draft data obtained from other sources such as the ASAE (1994). Unfortunately, much of the tillage implement draft data were obtained in the Midwest United States and Western Canada where soil texture and structure differ greatly from Québec soils. These soil-related differences are known to greatly affect soil mechanical behaviour (Angers 1990). Regional draft data are required for selected tillage equipment types to permit assessment of the applicability of the published draft data for tractor/implement matching under local conditions. A portable and low cost dynamometer is required for measurement of drawbar force components in an "on farm" research program.

LITERATURE REVIEW

A wide variety of draft dynamometers have been developed in the past. These can be classified into four categories: integral drawbar transducers (Self et al. 1987; Musonda and Bigsby 1985), instrumented hitch pins (Zoerb et al. 1983), link transducers (discussed by Zoerb et al. 1983), and three point-hitch dynamometers (Johnson and Voorhees 1979; Smith and Barker 1982; Palmer 1992; Thompson and Shinners 1989). Each dynamometer category has its own merits and drawbacks

and has often been designed for very specific applications. Integral drawbar transducers maintain the original hitch location, but reduction of drawbar cross sectional area to increase sensitivity results in loss of drawbar robustness. Link transducers are simple to fabricate, but most self align and only measure resultant drawbar force. Instrumented hitch pins can be used on a variety of tractors, but elliptical shaped holes in the drawbar and implement clevis resulting from normal wear can affect sensitivity (Personal communication, G.C. Zoerb, Professor Emeritus, Agricultural and Bioresource Engineering, University of Saskatchewan, Saskatoon, SK). Three-point hitch dynamometers are not suitable for trailed implements.

The extended octagonal ring (EOR) transducer is a robust device and is capable of independent measurement of forces in two dimensions and a moment in one dimension; consequently, it is an attractive option for use in a drawbar dynamometer. The EOR is a variation of the extended ring transducer; both devices feature a large central section where loading fixtures can be attached (Fig. 1). External loads produce bending in the thin ring sections, and the resulting ring strains are measured with strain gages.

Hoag and Yoerger (1975) derived analytical equations for bending moments in the ring sections of an extended ring transducer using strain energy techniques. As analytical equations are not available for the EOR with varying ring thickness, some researchers used the Hoag and Yoerger equations as an approximation for bending moment in the EOR. Unfortunately, the equation for bending moment in the left hand ring (Eq. 44 in Hoag and Yoerger 1975) has several typographic errors including an incorrect sign. McLaughlin (1996) presented the correct equations. In this paper, references to these equations will be the original authors (Hoag and Yoerger 1975), but the reader is reminded to check McLaughlin (1996) for the correct form of Hoag and Yoerger's Eq. 44.

$$M_\Theta = F_V \frac{R}{2}\left(\frac{2}{\pi} - \sin\theta\right) + F_D \frac{R}{2}\cos\theta + \frac{M_Z\left[\left(2+\frac{R\pi}{2L}\right) - \left(\frac{2R}{L}+\pi\right)\sin\theta\right]}{8+\frac{R\pi}{L}+\frac{2L\pi}{R}} \quad 0<\theta<\pi \qquad (1)$$

$$M_\Theta = F_V \frac{R}{2}\left(\frac{2}{\pi} - \sin\theta\right) - F_D \frac{R}{2}\cos\theta - \frac{M_Z\left[\left(2+\frac{R\pi}{2L}\right) + \left(\frac{2R}{L}+\pi\right)\sin\theta\right]}{8+\frac{R\pi}{L}+\frac{2L\pi}{R}} \quad \pi<\theta<2\pi \qquad (2)$$

$$\varepsilon_\Theta = \frac{6M_\theta}{Ebt^2} \qquad (3)$$

where:

- b, t, R = ring width, thickness, and mean radius (m),
- L = one half distance between ring centres (m),
- E = modulus of elasticity (Pa),
- θ = angle, measured clockwise from the top of ring (radians),
- M_θ = bending moment in ring at angular position θ (N m),
- ε_θ = flexural strain at angular position θ on ring (m/m),
- M_Z = applied external moment (N m), and
- F_D, F_V = applied draft and vertical loads (N).

Equations 1 and 2 are equivalent to Eqs. 43 and 44 in Hoag and Yoerger (1975) with the errors in Eq. 44 corrected and have been transformed to be consistent with the conventions for forces and moments used here: positive draft is to the right; positive vertical is downward; positive external moment is clockwise; and positive M_θ tends to open or increase the radius of curvature of the ring (Fig. 1).

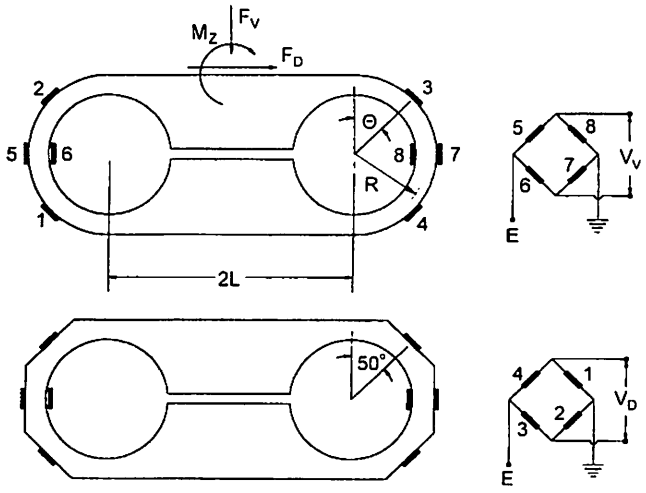

Fig. 1. Schematic representation of a plain extended ring (top) and extended octagonal ring, EOR (bottom), with characteristic dimensions, applied force systems, and strain gage positions for draft and vertical force measurement.

Leonard (1980) and Tessier et al. (1992) used two EORs mounted on either side of the tractor drawbar to measure both vertical and draft loading. Leonard (1980) placed the hitch point in line with the centres of the two EORs, while Tessier et al. (1992) placed the hitch point behind the centre of the two EORs to create differential draft loading on the two EORs when the dynamometer was subjected to lateral force components, thereby, achieving full three dimensional (3-D) load measurement capability. Although Tessier et al. (1992) found a linear relationship between lateral loading and differential outputs from the two EORs in the Double Extended Octagonal Ring (DEOR) configuration, this relationship was not in agreement with a simple force analysis. It was hypothesized that the torsional rigidity of the two EORs about the vertical axis combined with the semi-rigid bolt joint attaching the two

EORs to the loading fixture was responsible for this discrepancy. It was feared that dynamic loading in field conditions might alter the moment transmitting characteristics of the bolted joint resulting in a loss in accuracy of side load calibrations. Also, the 300 mm spacing between the two EORs provided insufficient clearance for clustered hitches common to many trailed harrows and cultivators.

OBJECTIVES

As no published dynamometer design completely satisfied our drawbar force measurement needs for a variety of implement types on a variety of producer owned tractors, the overall objective of this project was to develop a reliable 3-D drawbar force dynamometer. As a follow up to our previous endeavors (Tessier et al. 1992), the specific objectives of this research were to:

1. Develop a reliable 3-D drawbar transducer capable of measuring draft, vertical, and side loads for a variety of implements including cluster type hitch configurations and on a variety of tractors.
2. Develop calibration methods and predictive equations that could accommodate any cross sensitivity between draft, vertical, and side loads.

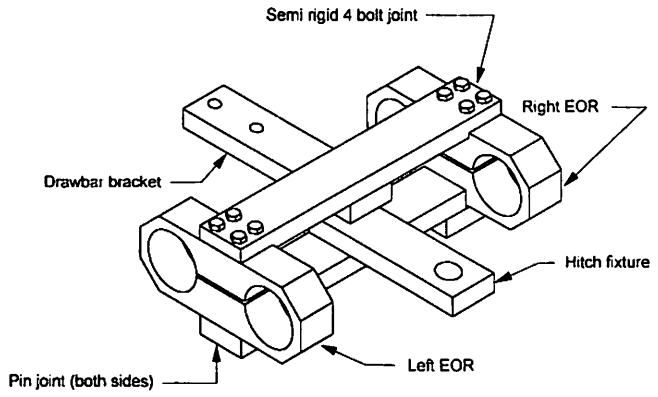

Fig. 2. Diagram of DEOR drawbar dynamometer with protective shrouds removed.

MATERIALS AND METHODS

Description

The design utilized two EORs each mounted on opposite sides of the drawbar (Fig. 2). Each EOR was attached to the upper drawbar bracket with four 9.5 mm diameter bolts and the drawbar bracket was bolted to the tractor drawbar. The hitch fixture was attached to the lower side of each EOR by a single 20 mm diameter bolt forming a pin joint. A sleeve 0.4 mm longer than the thickness of the hitch fixture was inserted in each bolt hole in the hitch fixture to support the clamping force of the bolt thereby eliminating clamping friction between the hitch fixture and the EORs (Fig. 3). This pin joint allowed a slight rotation of the hitch fixture about the vertical axis without transmitting moments to the EORs. The width of the hitch and drawbar fixtures where they contacted the EORs were both less than 2(L-R) (see Fig. 1) to avoid interference with the ring sections of the EORs as recommended by Godwin (1975).

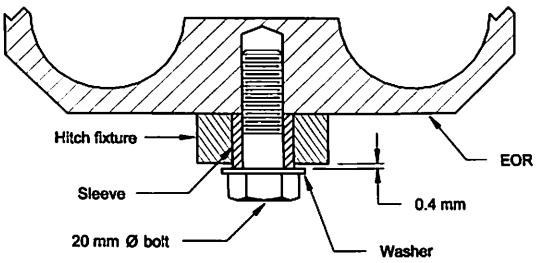

Fig. 3. Details of pin joint between hitch fixture and EORs.

The two EORs were separated by 356 mm (centre to centre) and the hitch point was positioned 152 mm to the rear of the pin joint connecting the EORs to the hitch fixture. These dimensions were chosen to provide adequate clearance for the large cluster hitches on some of the implements under study. Using elementary mechanics and a free body diagram of the hitch fixture (Fig. 4):

$$F_D = F_{D1} + F_{D2} \tag{4}$$

$$F_S = \frac{W}{2H}\left(F_{D1} - F_{D2}\right) \tag{5}$$

where:

W, H = dimensions of hitch fixture (Fig. 4) (m),
F_D, F_S = applied draft and side loads (N), and
F_{D1}, F_{D2} = applied draft loads on EORs 1 and 2, respectively (N).

Substituting dimensions of 356 and 152 mm for W and H, respectively, yields:

$$F_S = 1.17\left(F_{D1} - F_{D2}\right) \tag{6}$$

From Eq. 6, it is apparent that a side load applied at the hitch point results in a proportional differential draft load on the two EORs. This analysis is based on two important assumptions. First, the pin joints are assumed frictionless and permit a slight rotation of the hitch fixture about the vertical y-axis without transmitting moments to the EORs. This rotation of the hitch fixture results from a differential longitudinal (draft) deformation of the two EORs when the device is subjected to side loads. Second, it is assumed that bending stresses in the y-z plane imposed on the EORs by the side loads, F_{S1} and F_{S2} (Fig. 4), result in negligible strains on the horizontal or vertical strain gages on the EORs. This last assumption is based on the position of all strain gages on the EOR neutral axis (for bending in the y-z plane) and the high stiffness of the EOR in the y-z plane.

Design specifications

The design draft for the dynamometer was set at 45 kN and the design vertical load was set at 13 kN. As the hitch point was offset by 152 mm to the rear of the EOR centre (Figs. 2 and 4), the design vertical load acting at the centre of the hitch pin

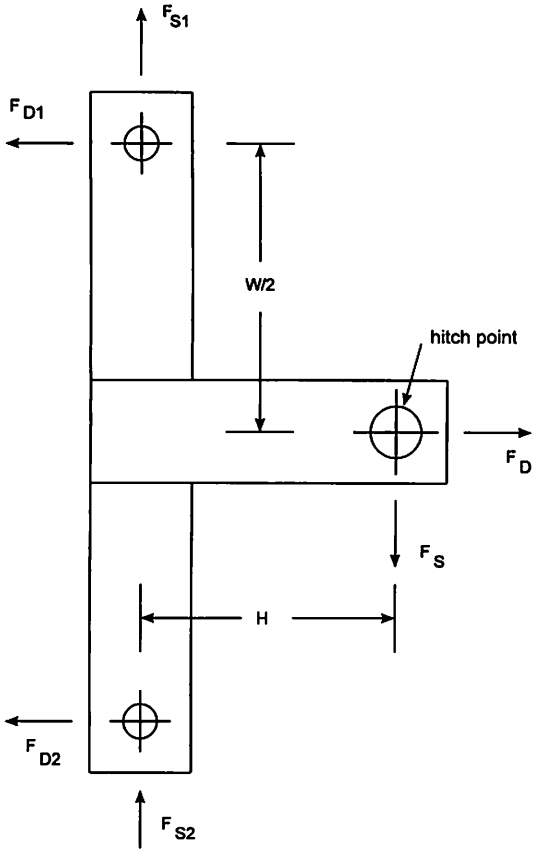

Fig. 4. Free-body diagram of the hitch fixture under draft and side load.

induces a moment, M_Z, of approximately 2 kN m on the DEOR. Because two EORs sustain the combined dynamometer loads, individual EOR design loads become one half of the above values. A maximum strain of 1500 με (μm/m) was set as a practical design limit to ensure long fatigue life of the strain gages and bonding cements (Measurements Group Inc. 1983). Considering a safety factor of 1.5 on draft measurements, each EOR was designed to undergo a maximum strain of 1000 με for an applied 22.5 kN draft force.

Sizing of the EOR

Strain gage locations of θ=50° and 90° (Fig. 1) were chosen for the horizontal and vertical strain gages, respectively, as suggested by Cook and Rabinowicz (1963). Ring strains at these two locations and at the design load were calculated for a number of combinations of ring thickness, width, and diameter using Eqs. 1, 2, and 3. As a result of this trial and error approach, dimensions of 12.7, 50.8, and 76.2 mm ring thickness, width, and inside diameter, respectively, and 356 mm EOR spacing (centre to centre) were chosen for the design. From Eqs. 1, 2, and 3, the peak strain at θ=50° for these EOR dimensions would be 1145 με for a draft load of 22.5 kN, and 1277 με for a combined 22.5 kN draft and 6.5 kN vertical force which also produces a 1.0 kN m pitch moment on each EOR. The side load was not considered in the original design. Although these strains were somewhat higher than the 1000 με, the EOR dimensions were retained as Eqs. 1, 2, and 3 were deemed conservative for EORs (Leonard 1980).

The EORs were machined from AISI 1020 steel (350 MPa yield stress). Micro Measurements CEA-06-125UW-350, strain gages were installed using M-bond 200 adhesive (Micro-Measurements Division, Measurements Group Inc., Raleigh, NC) following the manufacturer's recommended procedures (Measurements Group Inc. 1979). The strain gages were connected into separate four arm Wheatstone bridges for draft and vertical measurements (Fig. 1). Each EOR was covered by a sheet metal shroud to provide mechanical protection for the strain gages and associated wiring.

Calibration

A complete three-dimensional calibration was performed using an apparatus originally designed for calibration of a three-point hitch instrumentation system (McLaughlin et al. 1993). The DEOR dynamometer was mounted on a tractor drawbar and the tractor was rigidly secured to the loading apparatus to prevent tractor movement under high drawbar loads. Three independent hydraulic cylinders oriented along three orthogonal axes were used to apply, independently and simultaneously, draft, F_D, vertical, F_V, and side, F_S loads. Each hydraulic cylinder was fitted with a strain gage load cell for accurate measurement of the applied load. Maximum loadings were 36.5, 18.8, and 21.6 kN for the draft, vertical, and side forces, respectively. Side loading was applied in both directions, right and left, while both draft and vertical loads were applied in only one direction. Both uniaxial and fully combined loading calibrations were performed. Uniaxial loads were typically increased in steps of 10% of full load and applied in full loading-unloading cycles to facilitate checks for hysteresis. Fewer loading steps were used in combined loading.

The outputs of the strain gage bridges on the DEOR dynamometer and the three load cells were recorded with a Campbell Scientific 21X datalogger (Campbell Scientific Co., Logan, UT). A separate regulated 5 Vdc power supply was used to excite the bridges and outputs were recorded as for unbalanced Wheatstone bridges. The calibration data were first normalized by dividing the bridge output voltages by the bridge excitation voltage and the resulting data were subjected to multiple regression analysis (Steel and Torrie 1980).

Field evaluation

The DEOR dynamometer was used to measure drawbar forces exerted by a spring tine cultivator and a one-way discer within the scope of an on-going conservation tillage study. Fields were located in the St-Hyacinthe region, south-east of Montréal, QC on a Sainte Rosalie clay. Drawbar measurements were made for secondary tillage operations (first pass in the spring after fall plowing) at a nominal operating depth of 75 mm. The measurements were made over plots 30 m long by 15 m wide at a speed of approximately 5 km/h. Four replicates were used. The same datalogger used in the laboratory calibrations was also used for field measurements.

RESULTS AND DISCUSSION

Uniaxial calibration

Unfortunately, the DEOR assembly was seemingly overloaded during the initial uniaxial vertical calibration and the first loading curve (not shown) in both EORs exhibited an apparent yield initiating at approximately 13 kN, the design vertical

Table I. Primary, secondary, and cross sensitivity derived from uniaxial calibration data on the DEOR.

Loading axis	Primary sensitivity† ($\mu V\ V^{-1}\ kN^{-1}$)	Secondary sensitivity ($\mu V\ V^{-1}\ kN^{-1}$)	Cross sensitivity (Secondary/Primary) %
Draft	98.0	1.86	1.9
Vertical	94.8	6.59	7.0

†For draft loading, primary sensitivity is the response of the draft strain gage bridge while secondary sensitivity is response of the vertical bridge, and vice-versa for vertical loading.

for draft and vertical loading was 1.9 and 7.0%, respectively. Godwin (1975) found cross sensitivities of 1.1% and 2.1% for draft and vertical loads, respectively, when the draft gages were mounted at θ=34° and the loading fixture was confined to the central part of the boss section. Gu et al. (1993) reported varying cross sensitivity ranging from nearly 0 to 4.0% depending on the loading direction and noted a substantial increase in cross sensitivity when the EOR was loaded along the entire length of the boss face.

load. The first loading-unloading cycle exhibited significant hysteresis and a shift in the no-load zero. However, subsequent calculations using Eqs. 1, 2, and 3 indicated that the peak theoretical ring strain was well below the yield strain for the EOR material even with such overload. The cause of the hysteresis was not determined; it may have been yielding of residual stresses left from the machining process. Hysteresis was not apparent in subsequent calibrations and did not appear to affect the DEOR performance.

The device exhibited excellent linearity under uniaxial loading although the no-load intercepts were high (regression data not given). The high intercepts were expected since resistors were not added to balance the strain gage bridges after installation.

Primary, secondary, and cross sensitivity for each of draft and vertical loading were determined by regression analysis of the uniaxial loading calibration data (Table I). Cross sensitivity

Cross sensitivities reported for the DEOR in this paper are the cross sensitivities of the four arm bridge outputs as opposed to the cross sensitivity of strain at an individual gage location. In some of the literature, it is not clear whether the reported cross sensitivity is for strain at an individual gage location or for the output of a four arm strain gage bridge; thus, direct comparisons with the literature can not be made.

Combined loading calibration

A sequence of multiple regression models was developed for prediction of each of draft, vertical, and side load using combined loading calibration data (Table II). The first model in the sequence included only output from the primary strain gage bridge (draft bridge for draft load), the second model included both primary and secondary (vertical bridge for draft load), and the third model included primary, secondary, and interaction between the primary and secondary. The interaction term was not significant for draft loading and consequently, the third

Table II. Sequence of linear multiple regression prediction equations derived from three-dimensional calibration data on the DEOR. The prediction equations were derived from calibration data normalized to a 1.0 volt bridge excitation; output voltages of the DEOR bridges must therefore be divided by the excitation voltage before substituting into the prediction equations.

Prediction equation	SE of Residuals (N)	Regression coefficients			
		Draft, C_D ($N\ mV^{-1}$)	Vertical, C_V ($N\ mV^{-1}$)	Interaction, C_I ($N\ mV^{-2}$)	Intercept, b (N)
$F_D=C_DV_D+b$	770	-10,170 (28)*			-4134 (61)
$F_D=C_DV_D+C_VV_V+b$	359	-10,196 (13)	1,139 (26)		-2940 (39)
$F_V=C_VV_V+b$	880		-10,921 (64)		-3504 (80)
$F_V=C_VV_V+C_DV_D+b$	388	-658 (14)	-10,860 (28)		-4630 (43)
$F_V=C_VV_V+C_DV_D+C_I(V_D\ V_V)+b$	342	-383 (25)	-10,425 (43)	264 (21)	-4188 (52)
$F_S=C_D(V_{D1}-V_{D2})+b$	616	13,240 (27)			-6416 (30)
$F_S=C_D(V_{D1}-V_{D2})+C_VV_V+b$	582	13,257 (25)	-342 (42)		-6797 (55)
$F_S=C_D(V_{D1}-V_{D2})+C_VV_V+C_I(V_D\ V_V)+b$	543	12,858 (51)	-167 (44)	-348 (39)	-6581 (57)

*Standard errors of the regression coefficients are given in parenthesis.

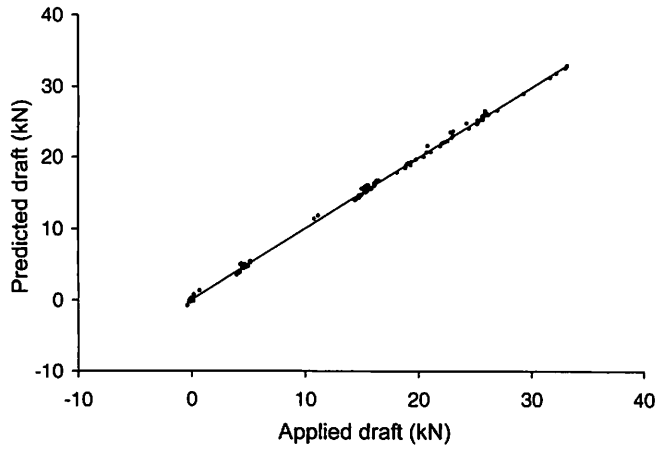

Fig. 5. Predicted draft load vs applied draft load using prediction equation developed from multiple regression on combined loading calibration data.

model for draft is not included in Table II. Applied and predicted draft, vertical, and side loads for the combined loading calibration are plotted in Figs. 5, 6, and 7, respectively. Predicted draft was calculated using the second draft model (Table II), while predicted vertical and side loads were calculated using the third vertical and side load models, respectively, which included the interaction term.

The prediction equations in the sequence show that the standard errors for both the residuals and the regression coefficients are substantially lower when cross sensitivity is accounted for by including output from both the vertical and horizontal strain gage bridges in the prediction equations. For example, the standard error of residuals for draft was reduced from 770 N, when only the draft bridge was included, to 359 N, when both the draft and vertical bridges were included in the prediction equation (Table II).

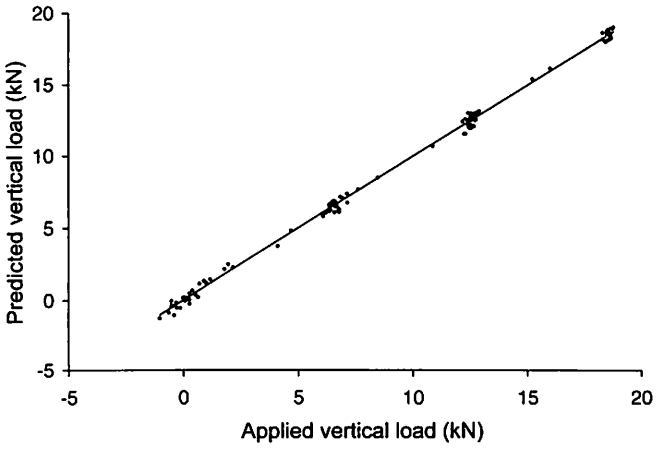

Fig. 6. Predicted vertical load vs applied vertical load using prediction equation developed from multiple regression on combined loading calibration data.

At heavy vertical loads, the DEOR assembly was noticeably sloped due to elastic deformation of both the drawbar and the drawbar bracket supporting the two EORs. Similarly, when strong side loads were applied, there was some rotation of the DEOR with respect to the drawbar. With the DEOR not in perfect alignment with the applied loads, the DEOR experienced a cross load component for each applied load and these extraneous cross loads showed up as apparent cross sensitivities in the DEOR output signals. As the DEOR, drawbar, and bolted joints are all approximately elastic, the magnitude of the DEOR misalignment and, therefore, cross sensitivity is proportional to the applied side and vertical loads. This explains the significant interaction terms in the vertical and side load prediction equations in Table II. In contrast, very little change in DEOR alignment occurred under draft loading and the interaction terms for the vertical loading were not significant. The large change in DEOR alignment under vertical load and negligible alignment change under draft load explains the large difference between the draft and vertical cross sensitivity as indicated in Table I.

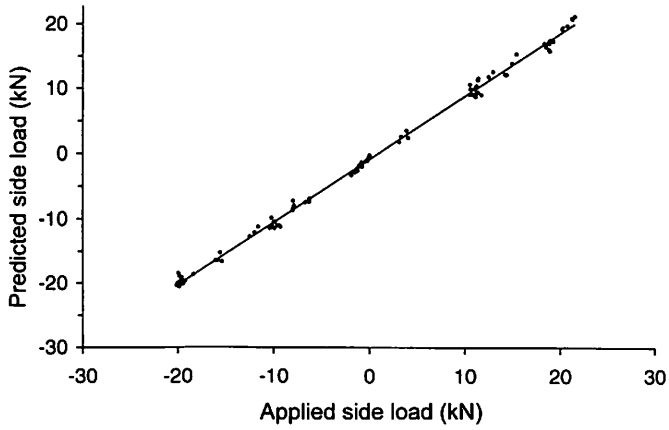

Fig. 7. Predicted side load vs applied side load using prediction equation developed from multiple regression on combined loading calibration data.

The multiple regression on three-dimensional combined loading calibration data successfully corrected for the rather large cross sensitivity as indicated by the standard errors of the residuals in Table II and the small scatter of the calibration data about the prediction curves (Figs. 5, 6, and 7). The combined loading used in our calibration simulated field loading more closely than the separate uniaxial loading such as used by Sime et al. (1992); thus, more confidence can be placed in the resulting prediction equations. Although the regression coefficients in Table II are applicable only to our DEOR, the multiple regression method of three-dimensional calibration is applicable to any design.

Sensitivity of the EORs calculated from Eqs. 1, 2, and 3 and elementary strain gage bridge theory (Gage Factor = 2.1) were respectively 109 and 65.5% of the bridge sensitivities of 98.0 and 94.8 $\mu V\ V^{-1}\ kN^{-1}$ for draft and vertical loading, respectively, determined from uniaxial calibrations. Leonard (1980) suggested that Eqs. 1, 2, and 3 are conservative, but our data indicate that Eqs. 1, 2, and 3 provide a reasonable estimate of stress at $\theta=50°$ but grossly under estimate stress at $\theta=90°$.

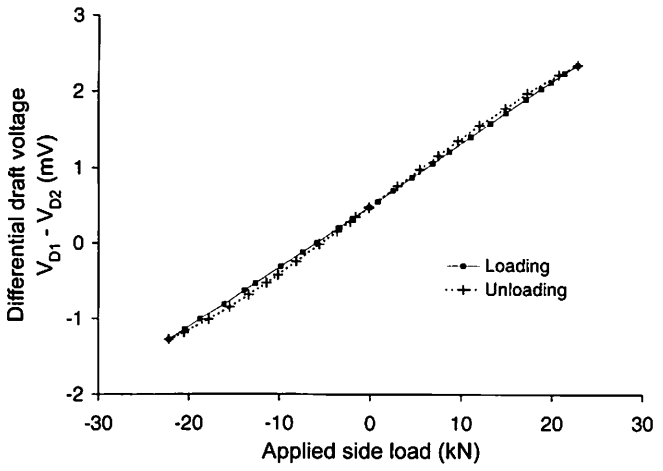

Fig. 8. Differential output of the draft bridges, V_{D1} - V_{D2}, on the two EORs vs applied uniaxial side load for a loading/unloading cycle.

Side loading response

The response curves for uniaxial side loading show relatively good linearity, but some loading-unloading hysteresis is apparent (Fig. 8). This hysteresis could be due to friction in the pin joints, both at the hitch point and between the hitch fixture and the EORs. For this DEOR geometry, the theoretical slope between the applied side load and the difference in draft for the two EORs was 1.17 (Eq. 6), while the measured slope was 1.19. In contrast, the geometry of our previous design with the semi-rigid bolted joints between the hitch fixture and the EORs yielded a theoretical slope of 1.0 (analyzing the four bolt joint as a pinned joint), while the slope calculated from calibration data was 1.88 (Tessier et al. 1992). Our present design with a pin joint resulted in performance much closer to the theoretical than the previous design with a four bolt joint which supports the hypothesis that the discrepancy in our previous design was due to moments being transmitted through the semi-rigid bolted joint.

The pin joint was considered successful in providing for differential draft loading of the two EORs under a drawbar side load. However, a drawbar vertical load applied at the hitch point 152 mm to the rear of the pin joint places a pitch moment on the joint creating a bending moment in the 20 mm diameter bolt which forms the pin joint. This is considered a weakness in the design and should be addressed in any further development.

The maximum strain calculated from Eqs. 1, 2, and 3 for draft, vertical, and side loads of 36.5, 18.8, and 21.6 kN, respectively, applied simultaneously during calibration of the DEOR was 3463 με and occurred at θ=180° in one EOR. This was well above the yield strain of about 1720 με for the EOR material. Except for the initial vertical load cycle, there was no apparent yielding of the EORs which would show up as a shift in the no-load bridge voltage after the calibration loads were removed. However, the EOR material may be very close to the yield strain with no safety factor left. Consequently, the DEOR capacity should be derated from the original design specifications, particularly under strong side loads which place additional draft load on one of the EORs. Side loads were not considered in the original design calculations. A more thorough investigation of maximum stress should be done with finite element analysis. Such analysis must consider the non-symmetric stress distribution in the four ring quadrants under combined loading.

Table III. Drawbar force components exerted by two secondary tillage implements operated at 75 mm depth at 5 km/h on a Ste-Rosalie clay as measured with the DEOR dynamometer.

Tillage Implement	Drawbar Force (kN/m width)		
	Draft	Vertical	Side
Spring Tine Cultivator (4.6 m)	3.95 (1.41)*	0.82 (0.24)	-0.06** (0.41)
One-way Discer (3.9 m)	3.24 (0.55)	0.74 (0.16)	2.06 (0.44)

* standard deviation of the measured load
** a negative sign indicates a side load to the right

Field performance

Increasing the spacing between the EORs by 102 mm and moving the hitch point 25 mm rearward over our previous design (Tessier et al. 1992) was sufficient to provide clearance for the large clevis hitches on the spring tine cultivators, even during the sharp turns imposed by typical tillage study field layouts.

Drawbar forces measured with the DEOR dynamometer for two secondary tillage implements are presented in Table III. Published values of draft for one-way discers (in clay soils) and spring tooth harrows (average over all soils) are 2.85 kN/m and up to 2.20 kN/m, respectively, (ASAE 1994) while CREAQ (1991) suggests values ranging from 4.5 to 9.7 kN/m, for spring tooth cultivators. The published values for the spring tooth cultivator are not very representative of those for a spring tine cultivator operated at 75 mm depth such as used in this field study. While the measured draft for the tillage equipment falls within the broad range outlined above, the notable difference confirms the need for revised draft values for Eastern Canadian conditions.

The ability of the DEOR dynamometer to measure side draft was demonstrated with the one-way discer. The measured side draft of 2.06 kN/m was large enough to affect tractor steering.

SUMMARY AND CONCLUSIONS

A drawbar transducer utilizing two Extended Octagonal Ring (EOR) transducers, one on each side of the drawbar, was developed for three-dimensional (3-D) force measurement. A hitch fixture was attached to the two EORs with pin joints and the hitch point was located behind the EORs such that side loads at the hitch point created differential draft loading in the two EORs. Drawbar draft and vertical load were calculated from the sum of the respective outputs of the two EORs, while side load was calculated from the difference of the draft output

of the two EORs. The spacings of the two EORs in the DEOR configuration was sufficient to avoid the problem of interference from massive cluster hitches on some implements which we experienced with an earlier design.

The Double Extended Octagonal Ring (DEOR) sensitivity was 98.0 and 94.8 $\mu V\ V^{-1}\ kN^{-1}$ for draft and vertical loading, respectively. Cross sensitivity was 1.9% and 7.0% for draft and vertical loading, respectively. Cross sensitivity was successfully compensated for using prediction equations developed by multiple regression on data from combined loading calibrations.

Theoretical equations developed for plain extended ring transducers predicted draft and vertical sensitivities of 109 and 65.5%, respectively, of those obtained from calibrations. These equations also predicted peak strain for the worst case calibration load well above the yield strain for the EOR material, but except for the first loading cycle, yielding was not observed. This discrepancy suggests that the device capacity should be derated from the original design specifications, particularly under strong side loads, and that a more thorough stress analysis be done using finite element analysis. The DEOR geometry with the pin joints attaching the hitch fixture to the two EORs resulted in differential draft loading of the two EORs under drawbar side loads. This permitted drawbar side loads to be determined from the difference in draft loads of the two EORs. However, vertical drawbar loads place a bending moment on the 20 mm diameter bolt forming the pin and this problem should be addressed in future designs.

REFERENCES

Angers, D.A. 1990. Compression of agricultural soils in Québec. *Soil & Tillage Research* 18:357-365.

ASAE. 1994. Standard D497.2 - Agricultural machinery management data. In *ASAE Standards 1994*, 341-348. St-Joseph, MI: ASAE.

Chi, L., S. Tessier and C. Laguë. 1991. Modeling soil compaction by liquid manure spreading equipment with finite element method. CSAE Paper No. 91-410. Saskatoon, SK: CSAE.

Cook, N.H. and E. Rabinowicz. 1963. *Physical Measurement and Analysis*. Reading, MA: Addison-Wesley Publishers.

CREAQ. 1991. Références économiques en agriculture. Comité de références économiques en agriculture du Québec. AGDEX 740. Machinerie : Force requise, vitesse de travail et efficacité. Ministère de l'Agriculture, des Pêcheries et de l'Alimentation du Québec, Québec, QC.

Godwin, R.J. 1975. An extended octagonal ring transducer for use in tillage studies. *Journal of Agricultural Engineering Research* 20:347-352.

Gu, Y., R.L. Kushwaha and G.C. Zoerb. 1993. Cross sensitivity analysis of extended octagonal ring transducer. *Transactions of the ASAE* 36(6):1967-1972.

Hånkasson, I., W.B. Voorhees and H. Riley. 1988. Vehicle and wheel factors influencing soil compaction and crop response in different traffic regimes. *Soil & Tillage Research* 11:239-282.

Hoag, D.L. and R.R. Yoerger. 1975. Analysis and design of load rings. *Transactions of the ASAE* 19:995-1000.

Johnson, C.E. and W.B. Voorhees. 1979. A force dynamometer for three-point hitches. *Transactions of the ASAE* 23(2):226-227, 232.

Leonard, J.J. 1980. An extended-octagon rigid drawbar dynamometer. *Agricultural Engineering Australia* 9(1):3-8.

McLaughlin, N.B. 1996. Correction of an error in equations for extended ring transducers. *Transactions of the ASAE* 39(2):443-444.

McLaughlin, N.B., L.C. Heslop, D.J. Buckley, G.R. St-Amour, B.A. Compton, A.M. Jones and P. Van Bodegom. 1993. A general purpose tractor instrumentation and data logging system. *Transactions of the ASAE* 36(2):265-273.

Measurement Group Inc. 1979. Strain gage installations with M-Bond 200 adhesive. Instruction Bulletin B-127-9. Measurement Group Inc., Raleigh, NC.

Measurement Group Inc. 1983. Strain gage selection. Technical note TN-505. Measurement Group Inc., Raleigh, NC.

Musonda, N.G.B. and F.W. Bigsby. 1985. Integral drawbar dynamometer. *Canadian Agricultural Engineering* 27(2):59-62.

Palmer, A.L. 1992. Development of a three-point-linkage dynamometer for tillage research. *Journal of Agricultural Engineering Research* 52(3):157-167.

Plouffe, C., S. Tessier, D. Angers and L. Chi. 1994. Computer simulation of soil compaction by farm equipment. *Journal of Natural Resources and Life Science Education* 23:27-34.

Raghavan, G.S.V. and E. McKyes. 1990. Interactions entre façons culturales, cultures et tassement du sol en vue de la conservation du sol et d'un rendement optimum. In *Pratiques culturales pour conserver le sol*, ed. S. Tessier. Université Laval, Québec, QC..

Self, K.P., J.D. Summers and G.L. McLaughlin. 1987. Instrumentation for determining four-wheel drive tractor performance. ASAE Paper No. 87-1629. St. Joseph, MI: ASAE.

Sime, M., S.K. Uphadhyaya and S. Pettygrove. 1992. Draft and energy requirements for no-till planters. ASAE Paper No. 92-1026. St. Joseph, MI: ASAE.

Smith, L.A. and G.L. Barker. 1982. Equipment to monitor field energy requirements. *Transactions of the ASAE* 25(5):1556-1559.

Steel, R.G.D. and J.A. Torrie. 1980. *Principles and Procedures of Statistics, a Biometrical Approach*, second edition. Montreal, QC: McGraw Hill Inc.

Tessier, S., A. Guilbert, N. McLaughlin and D. Tremblay. 1992. A double EOR drawbar pull transducer for 3-D forces measurements. CSAE Paper No. 92-406. Saskatoon, SK: CSAE.

Tessier, S., C. Laguë, R. Lambert, P. Tremblay and Y. Brochu. 1991. Soil compaction by liquid manure tanker. CSAE Paper No. 92-406. Saskatoon, SK: CSAE.

Thompson, N.P. and K.J. Shinners. 1989. A portable instrumentation system for measuring draft and speed. *Applied Engineering in Agriculture* 5(2):133-137.

Zoerb, G.C., N.G. Musonda and R.L. Kushwaha. 1983. A combined drawbar pin and force transducer. *Canadian Agricultural Engineering* 25(2):157-161.